Radiolytic approach for efficient, selective and catalyst-free CO2 conversion at room temperature

Changjiang Hu, Sarah Al Gharib, Yunlong Wang, Pingping Gan, Qiuhao Li, Sergey A Denisov, Sophie Le Caër, Jacqueline Belloni, Jun Ma, Mehran Mostafavi

Radiolytic Approach for Efficient, Selective and Catalyst-free CO_2 conversion at room temperature

Changjiang Hu,[a†] Sarah Al Gharib,[b†] Yunlong Wang, [a] Pingping Gan,[a] Qiuhao Li,[a]

Sergey A. Denisov, [b] Sophie Le Caer,[c] Jacqueline Belloni,[b] Jun Ma,[a*] Mehran Mostafavi [b*]

† Both Changjiang Hu and Sarah Al Gharib are considered as first authors.

[a] C.J. Hu，Y.L. Wang, P.P.Gan, Q.H.Li, Prof.J.Ma.
Department of Materials Science and Technology,
Nanjing University of Aeronautics and Astronautics, Nanjing 211106, China
E-mail: junma@nuaa.edu.cn

[b] Dr S. Al Gharib, Dr S. A. Denisov, Dr J. Belloni, and Pr M. Mostafavi
Institut de Chimie Physique CNRS-Université Paris-saclay, Orsay, France

[c] Dr S. Le Caer NIMBE, UMR 3685 CEA, CNRS, Université Paris-Saclay, CEA Saclay 91191 Gif-sur-Yvette Cedex, France

Abstract: The present study proposes a new approach for direct CO_2 conversion using primary radicals from water irradiation. In order to ensure reduction of CO_2 into $CO_2^{-\bullet}$ by all the hydrated electrons, we use formate ions to scavenge simultaneously the parent oxidizing radicals $H^\bullet$ and $OH^\bullet$ producing the same transient $CO_2^{-\bullet}$ radicals. Conditions are optimized to obtain the highest conversion yield of CO_2. The goal is achieved under mild conditions of room temperature, neutral pH and 1 atm of CO_2 pressure. All the available radicals are exploited for selectively converting CO_2 into oxalate that is accompanied by H_2 evolution. The mechanism presented accounts for the results and also sheds light on the data in the literature. The radiolytic approach is a mild and scalable route of direct CO_2 capture at the source in industry and the products, oxalate salt and H_2, can be easily separated.

Introduction

The excessive anthropometric carbon dioxide (CO_2) emission, that is responsible for climate changes, has led to worldwide efforts for a drastic diminution of its atmosphere level. Beyond the progressive abandonment of fossil fuels and the storage and sequestration of CO_2 surplus, the alternative strategy has been actively developed for efficient and cost-effective CO_2 conversion into other eco-friendly and value-added chemicals. [1-3]

Due to CO_2 chemical stability, the existing methods of its conversion into less oxidized

chemical species typically require a source of energy (i.e., heat, light, or electricity) to drive one- or multiply electron transfer reactions. For example, the reduction of CO_2 by coal to form CO occurs at very high temperature (> 700 °C) due to a large positive reaction enthalpy ($\Delta H°_{298\ K}$ = 172 kJ mol^{-1}).[4] The use for CO_2 reduction electron-rich chemicals, e.g. CH_4 and even H_2, also consumes significant amounts of energy, even in the presence of a catalyst.[5-7] The photocatalytic and electrocatalysis reduction of CO_2 using renewable energy resources likely accomplish the carbon neutral energy cycle while synthesizing fuels. However, their slow kinetics together with side reactions lead to a low efficiency and diverse products.[8,9] The newly -developed catalysis covering various matter-scales exhibits superior performance for CO_2 conversion,[10-12] but their ultimate practical viability is greatly hindered by several limiting factors such as high cost, lack of long-term stability, and upscale synthesis methodologies.[13] All these methods generally use multi-step processes based on complex chemistry, and essentially call for more direct and selective pathways.

The hydrated electron (e_{aq}^-) is the most powerful reducing species with a standard reduction potential of − 2.9 V_{NHE} that is larger than the reduction potential of CO_2 /$CO_2^{\bullet-}$ (− 2.14 V_{NHE} in water). [14] Therefore, e_{aq}^- can reduce aqueous CO_2 at room temperature without any catalyst. By taking advantage of the e_{aq}^- chemistry, the approaches of electrochemistry,[15] and more recently photoelectrochemistry[16-18] have been developed to reduce CO_2, but with a low Faradaic efficiency.

Herein, we exploit high-energy ionizing radiation as a promising method for aqueous CO_2 reduction.[19] As the reducing radicals are directly formed in water at room temperature, this method is effective without requiring the use of any catalyst. However, up to now, the appropriated chemical conditions were not explored to enable maximizing CO_2 conversion yield. Indeed, the fast back-oxidation by the symbiotic $OH^\bullet$ radicals has to be eliminated which remains a challenge for the CO_2 conversion efficiency.

This work aims to reduce the aqueous CO_2 into $CO_2^{\bullet-}$, the key precursor of radiolytic products, by utilizing all primary radiation-induced water radicals. Among the few possible candidates to create the fully reducing conditions in irradiated aqueous CO_2 solutions, formate ions were chosen as $OH^\bullet$ and $H^\bullet$ scavengers instead of methanol[20] or other organic chemicals,[21] because in this case, the reaction product is the same $CO_2^{\bullet-}$ radical as in the reduction of CO_2 by e_{aq}^-. The oxidation reactions of formate by $OH^\bullet$ and $H^\bullet$ into $CO_2^{\bullet-}$ and its second-order decay have already been extensively studied.[22-28] However, this process is hindered by H^+-catalysis leading to $CO_2^{\bullet-}$ disproportionation back to formate and CO_2.[29] Therefore, the present radiolytic experiments of CO_2 reduction in presence of formate, under catalyst-free aqueous

environment, were first performed at 1 atmosphere at various pH and then extended to higher CO_2 pressure up to 30 atmospheres. Based on the stoichiometric radical yields values in water, we establish the reaction mechanism under various conditions in order to optimize the CO_2 conversion.

Experimental methods

Materials

The gases CO_2 (99.999%) and Ar (99.999%) were purchased from Air Liquide Industrial Gases Company or Nanjing Shangyuan Industrial gas plant. Sodium formate NaCOOH and formic acid HCOOH were purchased from Merck. Potassium oxalate NaC_2O_4 was obtained from Fluka, NaOH from Sigma Aldrich Chemistry and H_2SO_4 (98%) from Nanjing Chemical Reagent Co., Ltd). Aqueous solutions were prepared in deionized water (Millipore, resistivity 18.2 MΩ cm).

13 mL of the samples were saturated at 20 °C with CO_2 through the septum. The hydration of CO_2 into H_2CO_3 is weak: K ($[H_2CO_3]/[CO_2]$) = 10^{-2}. The pH was controlled by adequate addition of NaOH or HCO_2H before the saturation by CO_2.

γ-Irradiation and analysis

γ-radiolysis was carried out at room temperature under CO_2 atmosphere using a panoramic ^{60}Co source. The dose rate, measured by the Fricke dosimeter, was 8 kGy h^{-1} (1 Gy = 1 J kg^{-1}), and the doses were increased up to 60 kGy.

In the case of the experiments performed under pressure, a stainless-steel vessel was used at the Nanjing University. We found very small amount of CH_4 at high pressure and one of the reasons of this production could be the reaction at the surface of stainless steel. However, as the CH_4 amount is very low we neglect it. Moreover, the mechanism and the yield were deduced from the experiments obtained at one atmosphere in glass vessels where we did not find CH_4.

Irradiation was carried out with a 60Co source. The dose rate in the vessel was determined to be 0.49 kGy h^{-1}.

Oxalate ions are quantified thanks to their optical absorption spectra. Measurements were performed using a Hewlett-Packard spectrophotometer). The absorbance is measured at 250 nm (ε = 28 mol^{-1} L cm^{-1}) where the absorbance of formate anion is negligible (Figure SI-1). The sodium oxalate was also analyzed by high performance liquid chromatography (HPLC) (Figure SI-2), (Eclassical 3100 HPLC Dalian Elite Analytical Instruments) on a chromatographic

column Shodex Sugar SH1011 (8.0 × 300 mm × 5.0 μm) and the eluent was an aqueous solution of H_2SO_4 (0.025 mol/L) at a flow rate of 1 mL/min and 50 °C with a UV absorption detection.

The gases produced (H_2 and CO) were measured by a gas chromatography set-up (GC9790 II co. Fuli instruments) equipped with a thermal conductivity detector (TCD) for H_2 and a flame ionization detector (FID) for CO (Figures SI-3). To examine whether the CO arose from the ionization/excitation in the solution or in the headspace gaseous CO_2(g), control radiolytic experiments of CO_2(g) alone were performed (Figure SI-4). The contribution of the emitted CO from the gaseous decomposition is low (for example at 1 CO_2 atm it is less than 2% of the total amount including the solution) (Figure SI-4), which is consistent with earlier radiolytic studies of gas-phase reactions that are often characterized by low product yields. The CO measurements were then systematically corrected from the CO formation arising from irradiated CO_2(g) under the same conditions.

Results and Discussion

pH effects on radiolytic product yields at 1 atm CO_2

The amounts of oxalate, CO and H_2 are measured versus irradiation dose and pH in aqueous solutions under 1 atm of CO_2 (or 3.8×10^{-2} mol L^{-1} of CO_2). First, preliminary experiments performed without formate on the radiolysis of CO_2-saturated solutions showed that the oxalate yield is negligible, and the major product is H_2. The radiolytic yield of H_2, $G(H_2) \sim 0.4 \times 10^{-7}$ mol J^{-1}, is measured from the slope of the species amounts versus the absorbed dose (Figure SI-3).

In the presence of sodium formate (5×10^{-2} mol L^{-1}) as the $OH^{\bullet}$ and $H^{\bullet}$ radicals scavenger, the H_2 radiolytic yield, $G(H_2)$ decreases from 2.75×10^{-7} mol J^{-1} at pH 1 to 1.04×10^{-7} mol J^{-1} at pH 7. The G(CO) value at 1 atm CO_2 is very low at pH 7 and its maximum reaches 0.17×10^{-7} mol J^{-1} at pH 2 and 3 (Figure 1 right).

The oxalate concentration increases at all pH linearly with the dose (Figure 1 left). The $G(C_2O_4^{2-})$ value increases from 0.05×10^{-7} mol J^{-1} at pH 3 to 3.5×10^{-7} mol J^{-1} at pH 7 following an opposite trend compared to H_2 (Figure 1 right). Below pH = 3 no oxalate is observed in CO_2-saturated formate solutions.

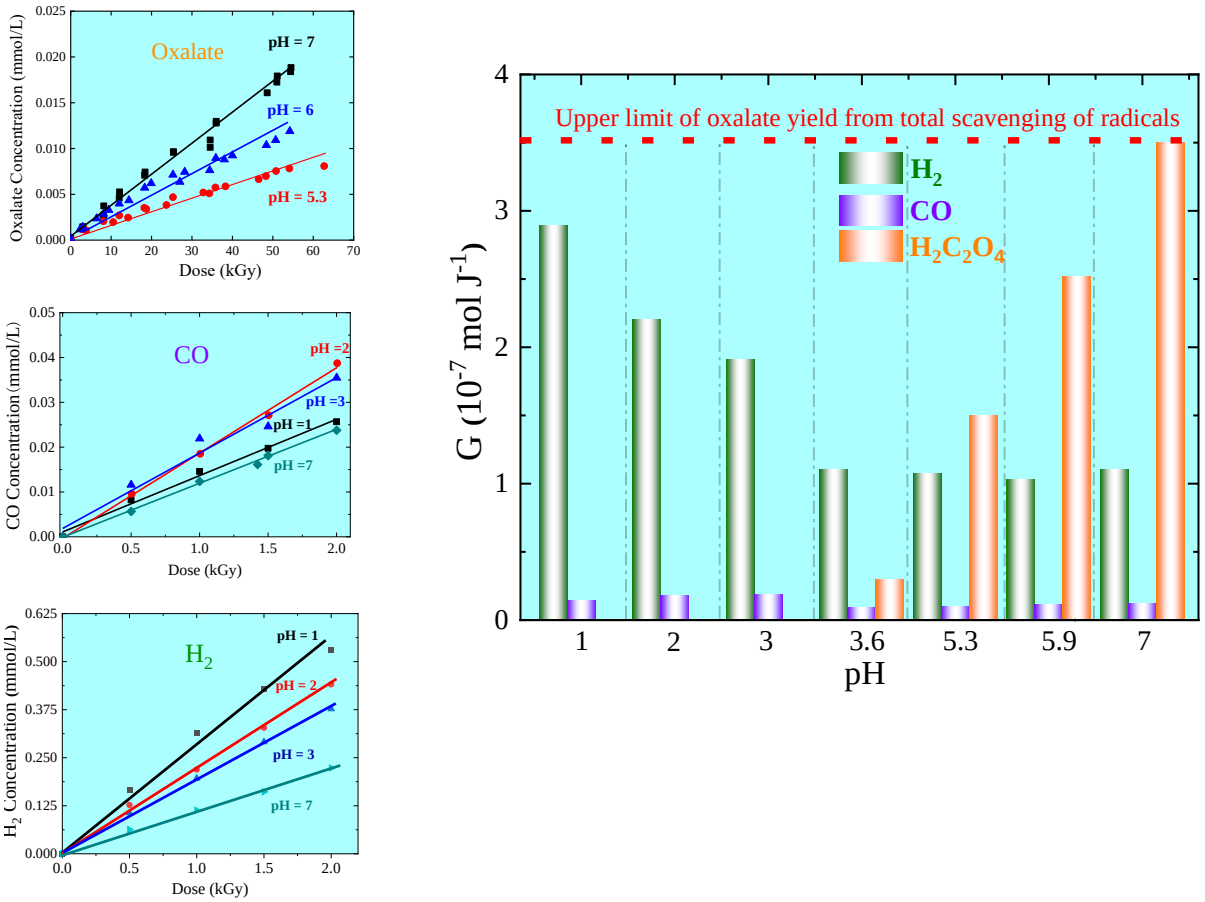

Figure 1. (Left) Representative measurements for the concentrations of oxalate (top), CO (middle) H_2 (bottom), *produced versus the irradiation dose at various pH.* ***(Right) Yields of H_2, CO and oxalate*** *in aqueous solution containing formate (5 $\times 10^{-2}$ mol L^{-1}) in the presence of CO_2 at 1 atm (the concentration of CO_2 in water is then 3.8 $\times 10^{-2}$ mol L^{-1}). Dotted line: Maximum oxalate yield, which is equal to ½ ($G(e_{aq}^-)$ + $G(H)^\bullet$ + $G(OH^\bullet)$) = 3.6 $\times 10^{-7}$ mol J^{-1} (see text)*

Around pH 7, according to the mechanism described below, the CO_2 consumption yield (G(-CO_2)) corresponds to about the formate consumption yield ($G(OH^\bullet)+G(H^\bullet)$), or to the formation yield of oxalate ($1/2(G(OH^\bullet) + G(H^\bullet) + (G(e_{aq}^-))$). Therefore, the CO_2 concentration after 60 kGy irradiation is estimated to be 1.3×10^{-2} mol L^{-1}. That represents 66% of the initial concentration that have been converted. By comparison, the decrease of the formate concentration is only 17%. In addition, the yields of H_2 and oxalate remain constant in this CO_2 concentration range. We also showed that $G(C_2O_4^{2-})$ is independent on $[HCO_2^-]$ from 5×10^{-2} to 10^{-1} mol L^{-1}. Therefore, these observations at very high doses indicate that the radiolytic approach is effective for sustaining CO_2 conversion in large amounts and that formate plays a significant role in the mechanism promoting the practicable and feasibility of this strategy.

CO_2 pressure effects on the radiolytic yields

The increase of the CO_2 pressure induces an increase of the CO_2 aqueous concentration, and thus an acidification of the solution. The final pH obtained after having imposed different values of CO_2 pressure can be calculated according to the various acid-base equilibria of the system for two initial pH (Figure SI-5).[30] Noteworthily, both HCO_3^- and CO_3^{2-} are present in solutions. However, the rate constants of the e_{aq}^- scavenging by these species ($k < 10^6\ M^{-1}\ s^{-1}$) are 3 orders of magnitude lower than that of reaction with CO_2. Therefore, HCO_3^- and CO_3^{2-} are omitted in the reaction mechanism.

In the absence of formate, in CO_2-saturated solutions, the substantial increase of the CO_2 concentration by the pressurization leads to the rise of G(CO) from 0 to 0.18×10^{-7} mol J^{-1} (30 atm, pH 5.3), but to a decrease of $G(H_2)$ from 0.4 to 0.1×10^{-7} mol J^{-1}, respectively (Figure SI-3). The oxalate yield $G(C_2O_4^{2-})$ is negligible. In the presence of formate, for final pH ranging from 3.9 to 3.2 for a CO_2 pressure varying from 1 to 30 atm, we observe a decrease of the H_2 yield and a marked increase of the CO yield without any oxalate formation (Figure 2 left).

For final pH around 7, the effect of CO_2 pressure on the yields of H_2 and CO presents similar trend as at pH 3. As shown above (Figure 1 Right), $G(C_2O_4^{2-})$ measured at 1 atm of CO_2 is the highest and equal to 3.5×10^{-7} mol J^{-1}. However, when the CO_2 pressure increases, $G(C_2O_4^{2})$ decreases down to a plateau value of 1.2×10^{-7} mol J^{-1} at 30 atm (pH 5.5) (Figure 2 Right). Obviously, in spite of a marked increase of the CO_2 concentration, the increasing acidity caused by pressurization leads to a decrease of the oxalate yield.

It is worthy to note that CO_2 pressure effects on decreasing $G(C_2O_4^{2-})$ and increasing G(CO) (Figure 2), are comparable to the pH effect observed at 1 atm pressure (Figure 1). However, the H_2 formation yield does decrease to lower values at higher CO_2 pressure (Figure 2) which is in contrast to the $G(H_2)$ increase when pH decreases at 1 CO_2 atm (Figure 1).

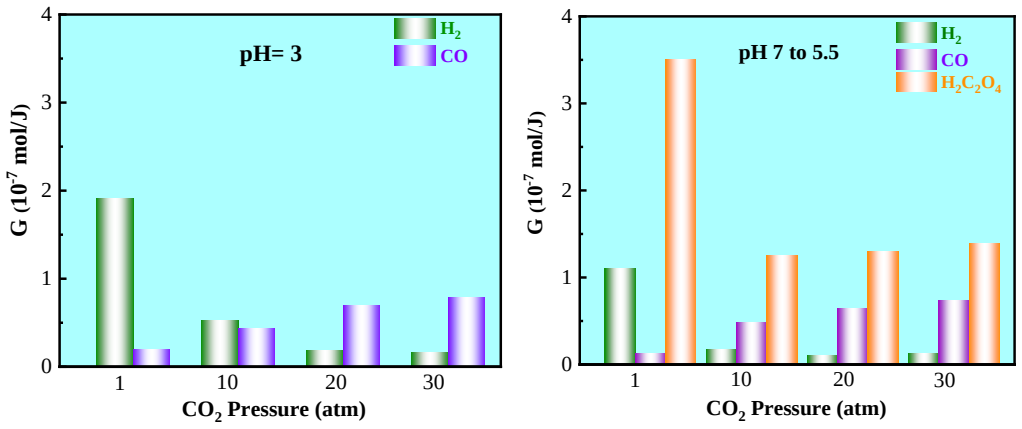

Figure 2. Radiolytic formation yields of H_2 and CO versus CO_2 pressure from 1 to 30 atm *(Left) in formic acid solution (pH 3). In these conditions, $G(C_2O_4^{2-})$ is negligible at any pressure. (Right) in solution containing initially 0.5 mol L^{-1} NaOH (final pH ranges from 7 to 5.5)*

Mechanism

Neutral medium, 1 atm CO_2

The generation of various species from water radiolysis at pH 7 is expressed as:

$$H_2O \rightsquigarrow e_{aq}^- (2.8),\ H^\bullet (0.62),\ H^+ (2.8),\ {}^\bullet OH (2.8),\ H_2 (0.42),\ H_2O_2 (0.73) \qquad (1)$$

(in brackets are the yields in 10^{-7} mol J^{-1} unit). [31, 32] These yields correspond to a scavenging factor of 10^7 s^{-1} (or 100 ns after the radical production and their mutual reactions in spurs). Note that the direct effect of radiation on CO_2 is negligible because of the low electron fraction (< 0.1) compared to water even at 30 atm pressure.

The reduction of CO_2 occurs through the reaction with e_{aq}^- (reaction 2 in Table 1). This reaction has been found to be almost controlled by diffusion ($k_2 = 8.2 \times 10^9$ $M^{-1}s^{-1}$),[20, 21,33] and the activation energy of k_2 between 5 and 200 °C was measured to be 15.9 kJ mol^{-1}. [20] The value of the rate constant k_2 warrants that all the solvated electrons reduce efficiently CO_2. The second-order reaction of dimerization of radicals $CO_2^{\bullet-}$ (reaction 3 in Table 1) into oxalate is in competition with the H^+-catalysed disproportionation (reaction 4 in Table 1) which leads to the formation of the initial reactants.[22-29]

In the absence of formate as an $OH^\bullet$ scavenger, the oxalate yield $G(C_2O_4^{2-}) = 0.02 \times 10^{-7}$ mol J^{-1}, is much less than $G(e^-_{aq})/2$. This very low yield and inefficiency of the process are most likely ascribed to significant loss of $CO_2^{\bullet-}$ caused by a secondary reaction with $OH^\bullet$ radicals (reaction 5 in Table 1) faster than their dimerization (reaction (3)). However, the $G(H_2)$ value is close to the primary H_2 yield $G(H_2) = 0.42 \times 10^{-7}$ mol J^{-1}.

Table 1. Reactions and corresponding rate constants *involved in the mechanism of $C_2O_4^{2-}$, H_2 and CO formation*

Reactions		**Rate constants (L mol^{-1} s^{-1}) at 20 °C**
$e^-_{aq} + CO_2 \rightarrow CO_2^{-\bullet}$	(2)	8.2×10^9 [20]
$CO_2^{-\bullet} + CO_2^{-\bullet} \rightarrow C_2O_4^{2-}$	(3)	1.4×10^9 [29]
$CO_2^{-\bullet} + CO_2^{-\bullet} + H^+ \rightarrow {}_2OC\text{-}CO_2H^{\bullet} \rightarrow CO_2 + HCO_2^-$	(4)	1.4×10^9 [29]
$OH^{\bullet} + CO_2^{-\bullet} \rightarrow OH^- + CO_2$	(5)	
$OH^{\bullet} + HCO_2^- \rightarrow H_2O + CO_2^{-\bullet}$	(6)	4.1×10^9 [22]
$H^{\bullet} + HCO_2^- \rightarrow H_2 + CO_2^{-\bullet}$	(7)	2.1×10^8 [31]
$e^-_{aq} + H^+ \rightarrow H^{\bullet}$	(8)	2.3×10^{10} [31]
$H^{\square} + CO_2^{-\square} \rightarrow CO + OH^-$	(9)	
$CO_2^{-\bullet} + CO_2 \rightleftharpoons [O_2C\text{-}CO_2]^{-\bullet}$	(10)	
$[O_2C\text{-}CO_2]^{-\bullet} + [O_2C\text{-}CO_2]^{-\bullet} + H^+ \rightarrow HCO_2^- + 3\,CO_2$	(11)	
$[O_2C\text{-}CO_2]^{-\bullet} + [O_2C\text{-}CO_2]^{-\bullet} \rightarrow C_2O_4^{2-} + 2\,CO_2$	(12)	
$CO_2 + e^-_{qf} \rightarrow CO_2^{-\bullet}$	(13)	
$[O_2C\text{-}CO_2]^{-\bullet} + [O_2C\text{-}CO_2]^{-\bullet} + H^+ \rightarrow CO + HCO_3^- + 2\,CO_2$	(14)	

In the presence of formate, at neutral pH, the H_2 yield corresponds to the sum of the primary yield $G(H_2) = 0.42 \times 10^{-7}$ mol J^{-1} in reaction (1) and of the scavenging yield of $H^{\bullet}$ radicals by formate ($G(H^{\bullet}) = 0.62 \times 10^{-7}$ mol J^{-1}) in reaction (7). The experimental value $G(H_2) = 1.04 \times 10^{-7}$ mol J^{-1} (Figure 1 right) is in fair agreement with this sum $G(H_2) + G(H^{\bullet})$ (Figure 3 and Table 2). That means that in addition to primary radiolytic H_2, all the $H^{\bullet}$ radicals are exploited to produce H_2.

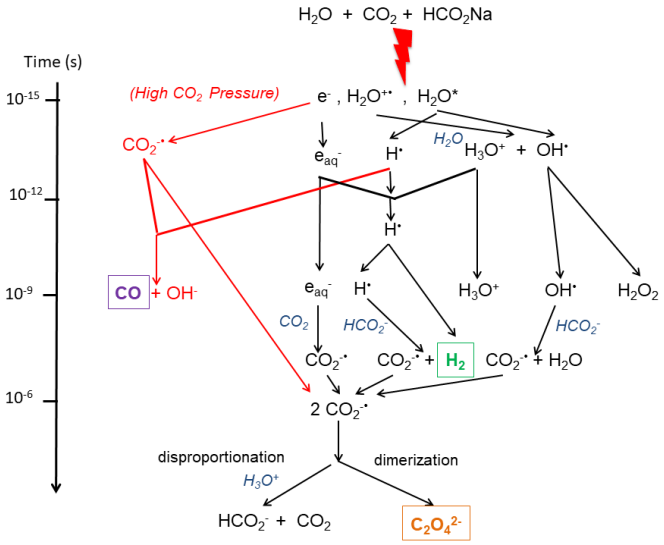

Figure 3. Scheme of the radiolysis of CO_2-saturated solutions of sodium formate. At pH 7 and 1 atm (in black), the $CO_2^{\bullet-}$ dimerization and the CO_2 conversion into oxalate are optimized: $G((C_2O_4^{2-})) = ½\ (G(e_{aq}^-) + G(H^\bullet) + G(OH^\bullet) = 3.5 \times 10^{-7}$ mol J^{-1} and $G(H_2) = (G(H^\bullet) + G(H_2)) = 1.04 \times 10^{-7}$ mol J^{-1}. At pH < 7, $G(C_2O_4^{2-})$ decreases because the H^+-catalyzed disproportionation of $CO_2^{\bullet-}$ is involved and becomes significant. At high CO_2 pressure (in red), CO_2 scavenges early the electrons before their hydration and the radicals $CO_2^{\bullet-}$ react with $H^\bullet$ radicals in spurs yielding CO. Simultaneously, the pH decrease favors the disproportionation, so that the oxalate yield becomes negligible. The arrow on the left indicates the time after the radiation-induced ionisation and excitation of the aqueous solution.

Table 2. Summary of product yields and predominant mechanisms *in the radiolysis of CO_2 solutions with sodium formate 5 × 10^{-2} mol L^{-1}. dispr and dim are the disproportionation and the dimerization of the precursor radical $CO_2^{-\bullet}$, respectively. Primary yields of species arising from water radiolysis are in italic.*

Irradiated Systems	$G(H_2)$ (10^{-7} mol J^{-1})	$G(CO)$ (10^{-7} mol J^{-1})	$G((CO_2)_2^{2-})$ (10^{-7} mol J^{-1})
CO_2 30 atm	0.16	0.7	0
pH 3	<< $G(H_2) + G(H^\bullet)_{acidic}$	= $G(H_2O^*)$	*Only dispr*
CO_2 30 atm	0.13	0.7	1.3
pH 5.3	<< $G(H_2) + G(H^\bullet)_{acidic}$	= $G(H_2O^*)$	*Competition dim/dispr*

CO_2 1 atm pH 3	2.0 $< G(H_2) + G(H^\bullet)_{acidic}$	0.14	0 *Only dispr*
CO_2 1 atm pH 5	1.0 $= G(H_2) + G(H^\bullet)_{neutral}$	0.08	1.5 *Competition dim/dispr*
CO_2 1 atm pH 7	1.04 $= G(H_2) + G(H^\bullet)_{neutral}$	0.08	3.5 $= ½ (G(e_{aq}^-) + G(H) + G(OH^\bullet))$ *Only dim*

Part of $CO_2^{\bullet-}$ produced in CO_2-saturated sodium formate solutions is due to the e_{aq}^- scavenging by CO_2 (reaction 2) and the other part is due to the scavenging of $OH^\bullet$ and $H^\bullet$ by formate (reactions 6 and 7). According to k_6 and k_7 values, and to the formate concentration, the scavenging half-time for reaction (6) is 4 ns and $G_{4ns}(OH^\bullet) \approx 3.3 \times 10^{-7}$ mol J^{-1}. [34, 35] Therefore, from reactions (2, 3, 5, 6 and 7), the maximum value of oxalate yield is $G(C_2O_4^{2-})_{calc} = ½ (G(e_{aq}^-) + G(H^\bullet) + G(OH^\bullet)) = 3.6 \times 10^{-7}$ mol J^{-1} (dotted line in Figure 1 Right), with $G_{4ns}(e_{aq}^-) = G_{4ns}(OH^\bullet) \approx 3.3 \times 10^{-7}$ mol J^{-1} and $G(H^\bullet) \approx 0.62 \times 10^{-7}$ mol J^{-1}. The experimental yield obtained at pH 7: $G(C_2O_4^{2-}) = 3.5 \times 10^{-7}$ mol J^{-1} is in excellent agreement with this maximum value. It is remarkable that under these mild conditions, the e^-_{aq} scavenging, which yields the conversion of CO_2 at 1 atm into oxalate, is complete and that the disproportionation path (4) is inactive. Indeed, in formate and CO_2 solutions, efficient reductive conditions of the aqueous solutions are fulfilled because, as an $OH^\bullet$ and $H^\bullet$ scavenger, formate inhibits the recombination reaction (5).[36,37] The scheme of the mechanism is summarized in Figure 3. The e_{aq}^- scavenging for selectively converting CO_2 into oxalate is completely exploited. Moreover, the $H^\bullet$ radical scavenging by formate yielding H_2, a useful fuel, is also complete. The efficiency of the absorbed radiation energy is thus 70% for the oxalate formation (32% for the reducing conversion of CO_2 and 38% for the formate oxidation),[38] plus 14.5% for the hydrogen formation.

Acidic medium

The yield of H_2 increases in acid medium at CO_2 atmospheric pressure (Figure 1) because e_{aq}^- are replaced by $H^\bullet$ radicals via reaction (8) and more $H^\bullet$ radicals are scavenged by formate (reaction (7)). Thus at pH 1 under 1 atm CO_2, the yield would be $G(H_2)_{calc} = G(H^\bullet)_{acidic} + G(H_2) = (3.42 + 0.42) \times 10^{-7}$ mol J^{-1}. However, the experimental value is lower: $(G(H_2)_{exp} = 2.8 \times 10^{-7}$

mol J^{-1}), showing that a small part of $H^{\bullet}$ radicals are thus lost in another reaction, such as the $CO_2^{\bullet-}$ radical reduction into CO (reaction (9)). This reaction may occur within the ionisation spurs before the homogenous dispersion of the radicals and explains the CO formation, although the experimental result is only $G(CO) = 0.17 \times 10^{-7}$ mol J^{-1}.

At 1 atm of CO_2, the oxalate yield $G(C_2O_4^{2-})$ decreases with the pH decrease (Figure 1). However, the simultaneous formation yield of the oxalate precursor $CO_2^{\bullet-}$ (either formed by reactions 2 or 6 and 7) is pH-independent. In a previous mechanistic study[29] of $CO_2^{\bullet-}$ arising from CO oxidation by $OH^{\bullet}$ (without CO_2), it was shown that at low pH the oxalate yield $G(C_2O_4^{2-})$ was strongly inhibited, and in contrast $G(CO_2)$ increased, owing to the disproportionation of $CO_2^{\bullet-}$ into CO_2 and formate (reaction 4). However, the rate constant of the second-order decay of $CO_2^{\bullet-}$ ($2k = 1.3 \times 10^9$ M^{-1} s^{-1}) is also pH-independent. They concluded that the disproportionation (4) was catalysed by protons and favored by the acid form $HCO_2^{\bullet}$ of the radical $CO_2^{\bullet-}$ (pK_a ($HCO_2^{\bullet}/CO_2^{-\bullet}$) ≈ 2.3). The protons would govern the disproportionation because of the presence of an intermediate head-to-tail adduct linking the carbon atom of one molecule to an oxygen atom of the other one. [29] Other values of $CO_2^{\bullet-}$ pK_a were proposed in the literature.[26, 27,39] However, the value recently determined by time resolved Raman spectroscopy measurements was $pK_a = 3.4$.[40]

We observe a more drastic influence of H^+ on the $G(C_2O_4^{2-})$ decrease than in ref.[29] (Figure 1). The main difference here to that study is the saturation of the solution by CO_2. The mechanism of the photoelectrochemical CO_2 reduction proposed by Tryk et al. [16] involves the reaction of the radical $CO_2^{\bullet-}$ with CO_2 forming, at least partially, the transient dimer radical anion $O_2C\text{-}CO_2^{-\bullet}$ (reaction 10). Various structures and stabilities of this dimer radical anion have been ab initio calculated.[41] Here we assume also that the dimer radical anion $O_2C\text{-}CO_2^{-\bullet}$ is formed under CO_2 atmosphere (reaction (10)). The fate of the dimer radical anion is not well known.[42] However, we propose that the dissociative disproportionation of $O_2C\text{-}CO_2^{-\bullet}$ radical (reaction 11) would be favored vs the dimerization (reaction 12). As it was recently suggested, the disproportionation of $O_2C\text{-}CO_2^{-\bullet}$ radical may also lead to CO formation (reaction 14).[43] Considering that the oxalate yield at a given pH is less in CO_2-saturated than in Ar-saturated formate solutions of ref 29, the carbon-carbon bonding in the dimer radical $O_2C\text{-}CO_2^{-\bullet}$ structure possibly inhibits a new addition and reorganization into the oxalate in contrast to reaction (4). Because the inflexion point of the oxalate yield increase is shifted to higher pH value than in conditions without CO_2, the pK_a ($O_2C\text{-}CO_2H^{\bullet}/O_2C\text{-}CO_2^{-\bullet}$) value is tentatively estimated at about 5.5 (Figure 1). As a result, the influence of protons in the H^+-catalysed disproportionation is stronger for $O_2C\text{-}CO_2^{-\bullet}$ (reaction 11) than for $CO_2^{-\bullet}$ (reaction 4).

Effects of high CO_2 pressure

The pressure increase induces also a marked concentration increase of CO_2 that scavenges rapidly in the radiation spurs the quasi-free electrons (e_{qf}^-) prior the hydration process (reaction (13)) as it was recently observed (Figure 3, red part).[30] In these conditions, the source of primary $H^\bullet$ radicals (reacting with formate and producing H_2, reaction 7) and of molecular hydrogen (reaction 1) progressively vanishes with the pressure increase. At pH = 3.9 to 3.2 for 1 to 30 atm respectively, we observe a decrease of the formation yield $G(H_2)$ to zero, and an increase of G(CO) (Figure 2). In contrast, the CO yield increases with the pressure because of the formation of CO via the reaction (9) between $CO_2^{-\bullet}$ and the $H^\bullet$ radicals issued from the dissociation of excited H_2O^* (Figure 3, red part). The $OH^\bullet$ radicals are still scavenged by formate and yield $CO_2^{-\bullet}$, but their H^+-catalysed disproportionation totally inhibits the formation of oxalate (Figure 3). Thus, the formation yield of oxalate is negligible under acidic conditions at any pressure.

In formate solutions initially added with 0.5 mol L^{-1} NaOH at increasing CO_2 pressure (final pH = 7 to 5.4 for 1 to 30 atm, respectively), the oxalate yield decreases from $G(C_2O_4^{2-}) = 3.5\times10^{-7}$ mol J^{-1} at 1 atm to a plateau at 1.3×10^{-7} mol J^{-1} at pressures > 10 atm (Figure 2). However, even if the part of $CO_2^{-\bullet}$ radicals, arising from the fast (reactions 2) and ultrafast (reaction 13) CO_2 reduction, increases versus the part arising from formate oxidation by $OH^\bullet$ scavenging (reaction 6), the total yield $G(CO_2^{-\bullet})$ does not change. Above 10 atm (pH 5.4), $CO_2^{-\bullet}$ radicals undergo only partly the dimerization into oxalate (reactions 3 and 12) because of the competition with the H^+-catalysed disproportionation (reaction (11)) (Figure 3 and Table 2)). In fact, the value of the yield $G(C_2O_4^{2-}) = 1.3\times10^{-7}$ mol J^{-1} at pressures > 10 atm (Figure 2) is close to the value at the same pH 5 at 1 atm (Figure 1). The effect of pH is thus more decisive than that of CO_2 concentration in the conversion into oxalate.

The mechanism proposed in the present study (Figure 3 and Table 2) could be also of interest for previous results. The e_{aq}^- chemistry contributing to scalable CO_2 reduction has recently attracted increasing attention for example in photoelectrocatalytic[17] or plasma[15] processes where the analogy with the initial reduction of CO_2 by e_{aq}^- in radiolysis was underlined. However, the main feature in these studies is that the symbiotic oxidizing species which are unavoidably formed together with e_{aq}^-, are responsible of back-reactions and low overall efficiencies of the reduction. In contrast, in the present radiolytic approach the oxidizing species are scavenged by formate, which is chosen to contribute moreover to a selective production of oxalate and H_2. The mechanism in Figure 3 and Table 2 explains how the radiation radicals are

used and the efficiency is thus optimized. Furthermore, the radiation-induced reduction method is an achievable**,** promising and scalable route for industrial CO_2 conversion. This method is promoted by the current availability of cost-effective industrial electron accelerators and ^{60}Co -γ sources. Though the aim of our work was not to give details on the economic aspect of this process and its possible valorization, it is known that the price of oxalate is higher than that of sacrificial formate. In addition, the valuable H_2 is produced during this process. Several parameters intervene in the calculation of the total cost of the CO_2 conversion. Eventually, our first estimation suggests that this simple process has a competitive energy cost compared to other chemical processes.

Conclusion

We demonstrated that the versatility of radiolytic pathways can be harnessed to direct the conversion of aqueous CO_2, 1 atm / HCO_2Na solutions at pH 7 at room temperature in order to produce value-added chemicals (oxalate, H_2) with optimized yields. All the radiolytic radicals are scavenged so that the radiation energy is significantly exploited for converting CO_2 into oxalate and H_2. The method does not require the presence of any catalyst. The knowledge of radiolytic yield values of water radicals was exploited in order to unravel the reaction mechanisms of all the processes at stake in the systems. The mechanism sheds light also on other previous results. Moreover, we suggest that the ionizing radiation delivered by irradiation facilities may be directly and easily coupled with an industrial source of CO_2. Therefore, the radiation-induced reducing radicals constitute a promising solution for the CO_2 conversion.

Acknowledgements

This work was supported by National Natural Science Foundation of China (Nos.11975122, 21906083), National Natural Science Foundation of Jiangsu Province (BK.2019030384) and Fundamental Research Funds for the Central Universities (N°. NE2020006).

Keywords: CO_2 conversion • Oxalate • CO_2 radiolysis • CO_2 reduction

[1] R. Snoeckx, A. Bogaerts, *Chem. Soc. Rev*. **2010**, *46*, 5805-5863.
[2] J. Albo, M. Alvarez-Guerra, P. Castaño, A. Irabien, *Green Chem*. **2015**,*17*, 2304-2324.
[3] R. M. Cue´llar-Franca, A. *J.* Azapagic, *CO_2 Util*. **2015**, *9*, 82–102.
[4] P. Lahijani, Z. A. Zainal, M. Mohammadi, A.R. Mohamed, *Renew. Sust. Energ. Reviews.***2015**, *41*, 615-632.
[5] J. Ma, N. Sun, X. Zhanga, N. Zhao, F. Xiao, W. Wei, Y. Sun , *Cat. Today*, **2019**,*148*, 221-231.
[6] A. Akhundi, A. Habibi-Yangjeh, M. Abitorabi, S. Rahim Pouran, *Cata. Rev. Sci. Eng*. **2019**, *61*, 595-628.
[7] B. Yao, T. Xiao, O. A. Makgae, X. Jie, S. Gonzalez-Cortes, S. Guan, A. I. Kirkland, J. R. Dilworth, H. A. Al-Megren, S. M. Alshihri, P. J. Dobson, G. P. Owen, J. M. Thomas, P. P. Edwards, *Nature Commun*. **2020**,*11*, 1-12.
[8] H. Ooka, M. C. Figueiredo, M. T. Koper, *Langmuir.* **2017**, *33*, 9307-9313.

[9] T. Burdyny, W. A. Smith, *Ene. Environ. Sci.* **2019**, *12*, 1442-1453.
[10] W. Tu, Y. Zhou, Z. Zou, *Adv. Mater.* **2014**, *26*, 4607-4626.
[11] Y. Y. Birdja, E. Pérez-Gallent, M. C. Figueiredo, A. J. Göttle, F. Calle-Vallejo, M. T. Koper, *Nature Energy.* **2019**, *4*, 732-745.
[12] H. Rao, L. C. Schmidt, J. Bonin, M. Robert*, Nature.* **2017**, *548*, 74–77.
[13] B. Hu, C. Guild, S. L. Suib, *J. CO_2 Util.* **2013**, *1*, 18-27.
[14] D. A. Armstrong, R. E. Huie, W. H. Koppenol, S. V. Lymar, G. Mere´nyi, P. Neta, B. Ruscic, D. M. Stanbury, S. Steenkenand, P. Wardman, *Pure Appl. Chem*. **2015**, *87*, 1139–1150.
[15] P. Rumbach, R. Xu, D.B. Go, *J. Electrochem. Soc*. **2016**, *163*, F1157–F1161.
[16] D.A. Tryk, T. Yamamoto, M. Kokubun, K. Hirota, K. Hashimoto, M. Okawa, A. Fujishima, *Appl. Organometal. Chem*. **2001**,*15*, 113-120.
[17] L. Zhang, Z. J. Zhao, T. Wang, J. L. Gong, *Chem. Soc. Rev.* **2018***, 47*, 5423–5443.
[18] L. Zhang, D. Zhu, G.M. Nathanson, R.J. Hamers, *Angew. Chem. Int. Ed.* **2014**, *126*, 9904-9908.
[19] M. M. Ramirez-Corredores, G. Gadikota, E. E. Huang, A. M. Gaffney, *Front. Energy Res*. **2020**, *8,* 108.
[20] A. Lisovskaya, D.M. Bartels, *Radiat. Phys. Chem*. **2019**, *158*, 61-63.
[21] N. Getoff, *Int. J. Hydrog. Energy.* **1994***, 19*, 667–672.
[22] A. J. Elliot, D.R. McCracken, G.V. Buxton, N.D. Wood, *J. Chem. Soc. Faraday Trans.* **1990,** *86*, 1539-1547.
[23] A. M. Lossack, E. Roduner, D.M. Bartels, *Phys. Chem. Chem. Phys.* **2001***, 3*, 2031-2037.
[24] P. Neta, M. Simic, E. Hayon, *J. Phys. Chem*. **1969**, *73*, 4207-4213.
[25] J. P. Keene, Y. Raef, A.J. Swallow, In Pulse Radiolysis (Eds.: Ebert, M., Keene, J.P., Swallow, A.J. Baxendale, H.J.), Academic Press, New York, **1965**, pp. 99-106.
[26] A. Fojtik, G. Czapski, A. Henglein, *J. Phys. Chem*., **1970**, *74*, 3204-3208.
[27] G. V. Buxton, R.M. Sellers, *J. Chem. Soc. Faraday Trans. 1*,**1973**, *69*, 555-559.
[28] M. Z. Lin, Y. Katsumura, Y. Muroya, H. He, T. Miyazaki, D. Hiroishi, *Radiat. Phys. Chem*., **2008**, *86*, 1208-1212.
[29] R. Flyunt, , M. N. Schuchmann, C. von Sonntag, *Chem. Eur. J.* **2001**. 7, 796-799.
[30] A. S. Denisov, M. Mostafavi, *Phys. Chem. Chem. Phys*. **2021**, *23*, 5804-5808.
[31] G. V. Buxton, C.L. Greenstock, W.P. Helman, A.B. Ross, *J. Phys. Chem. Ref. Data*,**1988**, *17*, 513−886.
[32] G. V. Buxton, **2008**. An overview of the radiation chemistry of liquids. In: M. Spotheim- Maurizot, M. Mostafavi, T. Douki, J. Belloni, (Eds.), Radiation Chemistry from Basics to Application in Material and Life Sciences. EDP Sciences-L'Actualité Chimique, Paris, pp. 3–16.
[33] S. Gordon, E.J. Hart, M.S. Matheson, J. Rabani, J.K.Thomas, *Disc. Farad. Soc*. **1963**, *36*, 193–205.
[34] A. K. El Omar, U. Schmidhammer, P. Jeunesse, J. P. Larbre, M. Lin, Y. Muroya, Y. Katsumura, P. Pernot, M. Mostafavi, *J. Phys. Chem. A*. **2011**,*115*, 12212-12216.
[35] F. Wang, U. Schmidhammer, J. P. Larbre, Z. Z., Zong, J. L. Marignier, M. Mostafavi, *Phys. Chem. Chem. Phys*. **2018**, *20*, 15671−15679.
[36] R.L. Willson, C.L. Greenstock, G.E. Adams, R. Wageman, L. M. Dorfman, Int. *J. Radiat. Phys. Chem*. **1971**, *3*, 211-220.
[37] P. Neta, R.H. Schuler, *J. Phys. Chem.* **1972**, *76*, 2673-2679.
[38] According to the ionization potential of water, each joule may ionize at maximum 10^{-6} mole of water.
[39] A.S. Jeevarjan, I. Carmichael, R. W. Fessenden*, J. Phys. Chem.* **1990***, 94,* 1372-1376.
[40] I. Janik, G. N. R. Tripathi, *J. Chem. Phys*. **2016,** *144*, 154307.
[41] S. H. Fleischman, K. D. Jordan, *J. Phys. Chem*. **1987**, *91*, 1300-1302.
[42] D. C. Grills, S. V. Lymar, *Phys. Chem. Chem. Phys.* **2018**, *20*, 10011-10017.
[43] H. Sheng, M. Hwan Oh, W. T. Osowiecki, W. Kim, A. P. Alivisatos, H. Frei, *J. Am. Chem. Soc*. **2018**,*140*, 4363−4371.